Wireless Pers Commun (2017) 95:4095–4111
DOI 10.1007/s11277-017-4044-3

Improved Nyquist-I Pulses to Enhance the Performance of OFDM-Based Systems

Shaharyar Kamal[1] · Cesar A. Azurdia-Meza[2] · Kyesan Lee[1]

Published online: 7 March 2017

Abstract Pulse shaping is used in orthogonal frequency division multiplexing (OFDM) based systems to reduce inter-carrier interference (ICI) power and peak-to-average power ratio (PAPR), which are considered the major weaknesses in OFDM-based systems. A novel family of Nyquist-I pulses called sinc exponential pulse (SEP) is proposed, and it is characterized by two new design parameters that provide extra degrees of freedom for a certain roll-off factor, α. SEP effectively decreases the relative magnitude of the two largest side lobes of the SEP frequency function, which minimizes the ICI power and reduces the PAPR in OFDM systems. Furthermore, the SEP possesses a broader main lobe, which provides sufficient improvement in bit-error-rate (BER). The behavior of the SEP is examined in the time and frequency domain by tuning its design parameters to obtain the sub-optimum SEP. Theoretical and simulation results show that the sub-optimum SEP performs better than other existing pulses in terms of ICI power, signal-to-interference ratio (SIR) power, BER, and PAPR in OFDM-based systems.

Keywords Frequency offset · Inter-carrier interference (ICI) · Nyquist-I pulses · OFDM · Pulse shaping functions · Peak-to-average power ratio (PAPR)

1 Introduction

Orthogonal frequency division multiplexing (OFDM) is a bandwidth-efficient communication technique that has emerged as the technology of choice for facilitating communication systems such as LTE Advanced, Wi-Fi, WPAN and WiMAX [1, 2]. The

✉ Kyesan Lee
kyesan@khu.ac.kr

1 Department of Electronics and Radio Engineering, Kyung Hee University, Suwon, Republic of Korea

2 Department of Electrical Engineering, University of Chile, Santiago, Chile

combination of OFDM and multiple-input multiple-output (MIMO) techniques as a single unit is being studied and proposed for the physical layer of 5G cellular networks. This combination can make important contributions to next-generation wireless communication systems [3, 4]. The extensive use of OFDM-based systems is due to various advantages; such as high data rate transmission capability, high bandwidth efficiency, and robustness to multi-path channel fading. On the other hand, OFDM systems are characterized by high peak-to-average power ratio (PAPR) values and high sensitivity to frequency offset.

The transmitted OFDM symbol is composed of multiple modulated subcarriers. The superposition of a large number of data subcarriers generates high power peak signals compared to the average signal power. In-addition, signals with large amplitude variations are characterized by high PAPR values [5]; therefore, an appropriate method for PAPR reduction is required to provide high-quality wireless networks.

Inter-carrier interference (ICI) is produced due to frequency offset, which degrades the performance of OFDM-based systems [6]. Frequency offset is produced by several factors, such as Doppler spread, difference in frequency between the transmitter and receiver oscillators, attenuation, and distortion in the channel. Several methods such as ICI self-cancellation schemes [7, 8], frequency domain equalization [9, 10], pilot insertion [11], receiver side windowing [12], and frequency error correction [13] have been proposed and investigated to reduce sensitivity to frequency offset in OFDM-based systems.

Pulse shaping is considered a suitable technique to reduce the ICI power [14–16] and PAPR [5, 17] in OFDM-based systems. Therefore, a novel family of Nyquist-I pulses is proposed in this manuscript, and it is referred as the sinc exponential pulse (SEP). The SEP is characterized by two new design parameters that provide additional degrees of freedom for a certain roll-off factor α. SEP is the product of an exponential expression and a modified similar raised-cosine (SRC) pulse. The SRC was initially proposed in [18] and modified in this manuscript. To fully validate the performance of the proposed SEP, other recently proposed were evaluated; such as the sinc parametric linear pulse (SPLP) and sinc parametric exponential pulse (SPEP) [19]. The evaluation was done in terms of terms of ICI power, signal-to-interference power ratio (SIR) power, PAPR, and bit-error-rate (BER) in OFDM systems. In general, the smaller side lobes of the SEP pulse will help to minimize ICI power [14] and reduce PAPR [5]. Further, a pulse with a broader main lobe contributes significantly to a decrease in BER [15].

1.1 Related Work

Several pulse shaping functions were studied and compared with the *better-than* raised cosine (BTRC) pulse [20, 21]. Numerous Nyquist-I pulses have been proposed and recommended for OFDM-based systems; such as the sinc power (SP) pulse [22], which is characterized by having an additional degree of freedom. The SP pulse performed better than the raised cosine (RC) pulse and the BTRC. The improved sinc power (ISP) pulse [14] is an enhanced version of the SP, which showed a great progress in ICI power and BER reduction. Furthermore, ISP with modified phase was analyzed in [15]. Phase modified sinc power (PMSP) pulse outperformed the ISP by providing smaller side lobes with a broader main lobe. Meanwhile, alternative pulses have been proposed, such as the improved modified Bartlett-Hanning (IMBH) windowing [23], which diminishes ICI power. Whereas the improved parametric linear combination (IPLCP) pulse [24] is used for PAPR reduction. In general, the IPLCP and IMBH pulses showed better performance than other existing pulses in terms of BER reduction. At the moment, IMBH and IPLCP are the best pulses in the literature for effectively dealing with the problem of sensitivity to frequency offset and PAPR in OFDM-based systems. However, the design and development of novel families of Nyquist-I pulses is a fundamental ongoing research topic due to increased demands for higher error-free data rates in next-generation wireless communication systems.

1.2 Contributions

The first contribution of this paper is to evaluate the proposed pulse using a roll-off factor of $\alpha = 0.22$. The 3rd Generation Partnership Project (3GPP) has suggested the use of $\alpha = 0.22$ for the pulse shaping filter at both sides of the transmitter and receiver of the user equipment (UE) and base station (BS) [25, 26]. Therefore, we consider $\alpha = 0.22$ throughout the manuscript in order to investigate its effect on the evaluated pulses.

Second, the robustness of the SEP in the time and frequency domain is analyzed by tuning the values of its design parameters i.e. γ and β. Investigations are made by varying γ while the constant β is fixed, and vice versa. This is because both parameters have a major impact on the proposed pulse.

Third, the SEP is compared with other recently proposed pulses by the authors of this manuscript, SPLP and SPEP [19]. The performance of the proposed pulse is also compared with other recently proposed pulses, such as IMBH [23] and IPLCP [24], in terms of ICI power, SIR power, BER, and PAPR in OFDM-based systems via numerical and theoretical simulations.

Finally, the pulse shaping function of the SEP has a simple design and expression, in comparison with other existing pulses. The average elapsed time of the convolution process that takes place between the modulated symbols and the pulse shaping function is measured, and is used as a metric of the complexity of the pulse.

The remainder of this paper is organized as follows. We describe the OFDM system model and present mathematical description of ICI, and SIR power in Sect. 2. The derivation of the proposed pulse and its performance with respect to time and frequency domain is discussed in Sect. 3. The comparisons of the proposed pulse with other existing pulses in terms of ICI power, SIR power, BER, and PAPR are presented in Sect. 4. Time complexity of the evaluated pulses is measured by taking the average elapsed convolution time given in Sect. 5. Concluding remarks are presented in Sect. 6.

2 OFDM System Model

Each OFDM symbol is the sum of N data symbols that are transmitted on orthogonal subcarriers using various modulation schemes; such as MPSK, and MQAM, as shown in Fig. 1. The complex data symbols become inputs to the Inverse Discrete Fourier Transform (IDFT); hence, each symbol is assigned to a particular orthogonal subcarrier. Then, the transmitted OFDM symbol is converted to a serial data stream, a digital-to-analog converter (DAC) is used along with a pulse shaping function. The time domain signal is then modulated at a particular carrier frequency, f_c. Finally, the complex time domain envelope of the OFDM symbol is transmitted through the channel and additive white Gaussian noise (AWGN) is added. At the receiver side, a reverse operation of the transmitter is applied.

At the receiver side, the input signal is converted to the digital domain using an analog-to-digital converter (ADC) along with a pulse shaping function to eliminate all frequencies

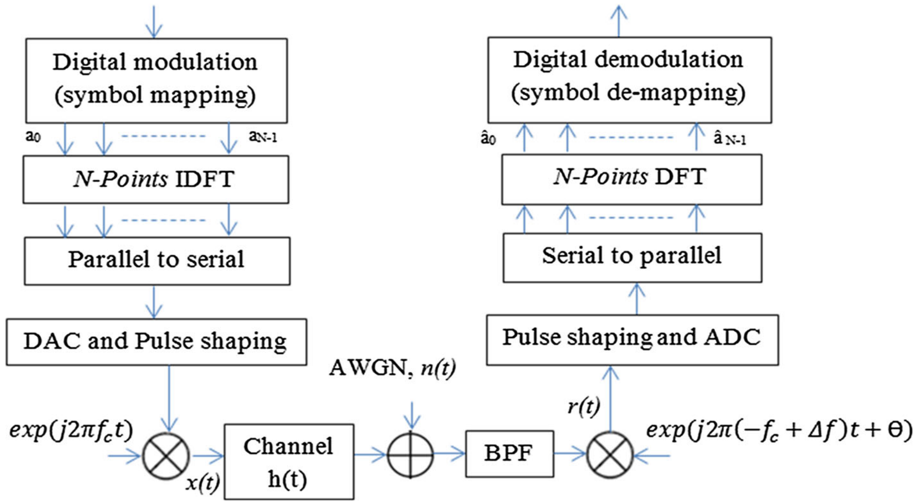

Fig. 1 *N*-subcarrier OFDM system model

above the Nyquist frequency. The Discrete Fast Fourier Transform (DFT) is used to analyze the signal in the frequency domain.

2.1 ICI and SIR Formulations

We followed the notations given in [21] to describe the ICI and SIR power in OFDM-based systems. The complex time-domain envelope of the transmitted OFDM symbol with the pulse shaping function is expressed as [27]

$$x(t) = \mathrm{Re}\left\{ e^{j2\pi f_c t} \sum_{k=0}^{N-1} a_k p(t) e^{j2\pi f_k t} \right\}, \tag{1}$$

where j is the imaginary unit, $\sqrt{-1}, f_c$ is the carrier frequency, f_k is the subcarrier frequency of the k-th subcarriers, $p(t)$ is the pulse shaping function that narrows or limits each data symbol for a certain interval of time, whereas a_k is the data symbol transmitted on the k-th subcarrier with zero mean and normalized average symbol energy. It is assumed that all data symbols are uncorrelated, and expressed as

$$E[a_k a_m^*] = \begin{cases} 1, \rightarrow k = m \\ 0, \rightarrow k \neq m, \end{cases} \quad k,\ m\ =\ 0, 1, \ldots, N-1, \tag{2}$$

where * represents a complex conjugate. To ensure the orthogonality of the subcarriers in an OFDM system, the following expression should be satisfied

$$f_k - f_m = \frac{k-m}{T}, \quad k, m = 0, 1, \ldots, N-1, \tag{3}$$

where $(1/T)$ is the minimum subcarrier frequency spacing that satisfies the orthogonality among the N-subcarriers. The received signal is expressed as follows

$$r(t) = x(t) \times h(t) + n(t). \tag{4}$$

where $h(t)$ is the impulse response of the channel, $\times$ represents the convolution between the transmitted signal and the channel impulse response, and $n(t)$ is the additive complex Gaussian noise. We assumed that $n(t)$ in (4) is AWGN with zero mean and variance $(N_0/2)$ per dimension in the channel. An ideal channel is assumed ($h(t) = \delta(t)$) to investigate the impact of the frequency offset, which is an approach commonly used in literature [14, 15, 19, 21, 22].

The distortion in the channel and frequency differences between the transmitter and receiver oscillators introduce carrier frequency offset Δf, and phase error θ. Hence, the received signal is given by Tan and Beaulieu [21]

$$r(t) = e^{j(2\pi\Delta f t+\theta)}\sum_{k=0}^{N-1} a_k p(t)e^{j2\pi f_k t} + n(t)e^{j(2\pi(-f_c+\Delta f)t+\theta)}. \tag{5}$$

According to Tan and Beaulieu [21], the decision variable for the transmitted symbol, a_m is

$$\hat{a}_m = \int_{-\infty}^{\infty} r(t)e^{-j2\pi f_m t}d_t. \tag{6}$$

The transmitted symbol can be decomposed using (3) and (6) as follows [21]

$$\hat{a}_m = a_m e^{j\theta}P(-\Delta f) + e^{j\theta}\sum_{\substack{k=0,\\ k\neq m}}^{N-1} a_k P\left(\frac{m-k}{T} - \Delta f\right). \tag{7}$$

The Fourier transform of the pulse shaping function $p(t)$, is denoted as $P(f)$. The power of the desired signal σ_m is defined as

$$\sigma_m = |a_m|^2|P(\Delta f)|^2, \tag{8}$$

whereas the ICI power is defined as [21]

$$\sigma_{ICI}^m = \sum_{\substack{k=0,\\ k\neq m}}^{N-1}\sum_{\substack{n=0\\ n\neq m}}^{N-1} a_k a_n^* P\left(\frac{k-m}{T} + \Delta f\right)P\left(\frac{n-m}{T} + \Delta f\right). \tag{9}$$

The average ICI power primarily depends on the frequency offset Δf, and the pulse shaping function $P(f)$. Furthermore, the average ICI power across different sequences is given in [21] as

$$\bar{\sigma}_{ICI}^m = \sum_{\substack{k=0,\\ k\neq m}}^{N-1}\left|P\left(\frac{k-m}{T}\right) + \Delta f\right|^2. \tag{10}$$

The signal-to-interference power ratio is represented as SIR, and for the *m-th* subcarrier is defined as [21]

$$SIR^m = \frac{|P(\Delta f)|^2}{\bar{\sigma}_{ICI}^m}. \tag{11}$$

3 Pulse Shaping Function

In OFDM-based systems, each data symbol is transmitted on a different subcarrier, allowing the data to be coded in the frequency domain. At the same time, the superposition of the subcarriers makes it difficult to analyze the behavior of the digital data in the time-domain, because we need to ensure that the subcarriers in the OFDM symbol maintain the orthogonality. A loss in orthogonality generates ICI and data loss. The most reliable method to recognize the state of the data in the frequency domain is to evaluate the inter-carrier interference (ICI) power in OFDM-based systems.

Each data symbol is transmitted on different orthogonal subcarriers using *P*(*f*), as shown in Fig. 2. The *P*(*f*) has to satisfy the Nyquist-I criterion to achieve zero interference among the subcarriers. A similar approach was utilized in [14, 15, 19, 21, 22, 24]. This fact can be implemented using (1) and (2), and expressed as

$$\int_{-\infty}^{\infty} p(t)e^{j2\pi(f_k - f_m)dt} = \begin{cases} 1, & \rightarrow k = m \\ 0, & \rightarrow k \neq m \end{cases}. \tag{12}$$

The *P*(*f*) requires spectral nulls at the frequencies $\pm 1/T$, $\pm 2/T, \ldots, \pm n/T$, which ensures the orthogonality of the subcarriers. Essentially, the expression defined in (13) represents the Nyquist-I criterion, but it is expressed in the frequency domain, and it is given as

$$P(f) = \begin{cases} 1, & \rightarrow f = 0 \\ 0, & \rightarrow f = \pm \frac{1}{T}, \pm \frac{2}{T}, \ldots \end{cases}. \tag{13}$$

We proposed a novel family of Nyquist-I pulses called sinc exponential pulse (SEP), which is characterized by two new design parameters, γ and β. Where γ is used to provide an extra degree of freedom by increasing the exponential power of the required function, and β is used to control the phase of the sinc function. The SEP is the multiplication of an exponential expression, which has the ability to diminish the side lobes, and a modified similar raised-cosine (SRC) pulse. The SRC pulse was initially proposed in [18], and

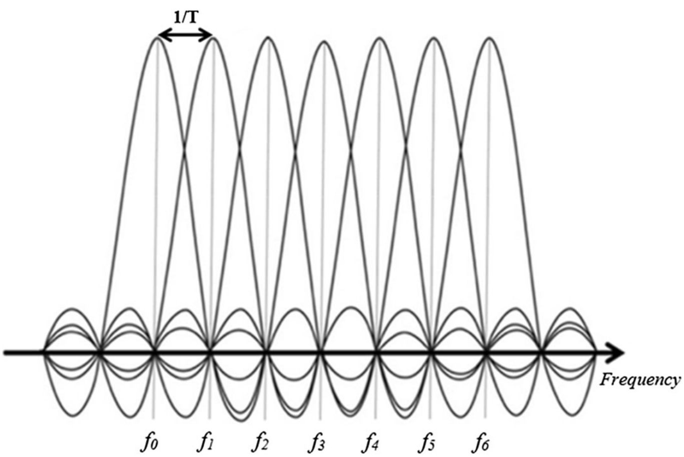

Fig. 2 OFDM signal spectrum

modified in this manuscript. The frequency response of the SEP is characterized by a closed-form expression, and it is given as follows

$$P_{SEP}(f) = \exp\{-\gamma(fT)^2\} \times \sin c(\beta fT)\frac{1 - 2\cos(\alpha\pi fT)}{(3\alpha fT)^2 - 1}, \quad (14)$$

In general, the SEP is characterized by three design parameters, including γ, β, and α. Parameters that provide extra degrees of freedom. The parameters γ and β are defined for all real numbers, whereas α is the roll-off factor and it is defined for $0 \leq \alpha \leq 1$.

In order to verify that the SEP satisfies the Nyquist-I criterion in frequency-domain, described in (13), the pulse proposed in (13) is evaluated for $f = 0$, and for any value of the parameters i.e. γ, β and α, is always equal to one. Furthermore, the SEP evaluated for $f = \pm\, 1/T$, $\pm 2/T,\ldots$, and for any value of the parameters i.e. γ, β and α, is always equal to zero. Therefore, we can say that the SEP, which is given in (14), fulfills the Nyquist-I criterion. We adjusted accordingly the new design parameters, γ and β, to analyze the behavior of the SEP in the time and frequency domain.

The comparisons of the frequency function of the SEP for different values of its new design parameters is presented in Fig. 3. The β value is fixed when the γ value varies, and vice versa. We observed that the side lobes of the SEP are nearly vanish as the values of γ and β increase. We took different values of γ and β as examples to show their significance with respect to the proposed pulse. In SEP, when β decreases, the main lobe wide increases, but when γ increases the magnitude of the two side lobes decreases. An increase in the value of β allows the main lobe to become narrow. This restricts the constant β to be equal to 2, which is the main reason a further increase in the value of β was not considered. Parameter $\gamma = 0.55$ is selected because it shows considerably broader main lobe and smaller side lobes. However, the optimum values of both parameters are discussed in detail in next section.

The behavior of the pulse shaping function in the time domain for the SEP with different values of γ and β is depicted in Fig. 4. A triangular waveform is observed for $\beta = 2$, which indicates a reduction in the amplitude of the function that narrows the OFDM symbol in a certain interval of time. However, such scenery reduces the ICI power and increases the SIR, but produces higher BER values [24]. This is why time-domain rectangular like waveforms are more desirable than triangular like waveforms [23, 24]. In triangular time-domain like waveforms, a pulse may not be able to limit the symbol

Fig. 3 Frequency function of SEP for $\alpha = 0.22$, with $\beta = 1$ when γ varies, and $\gamma = 0.55$ for $\beta = 2$

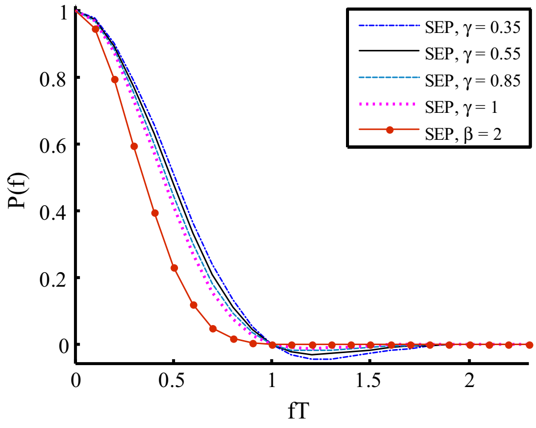

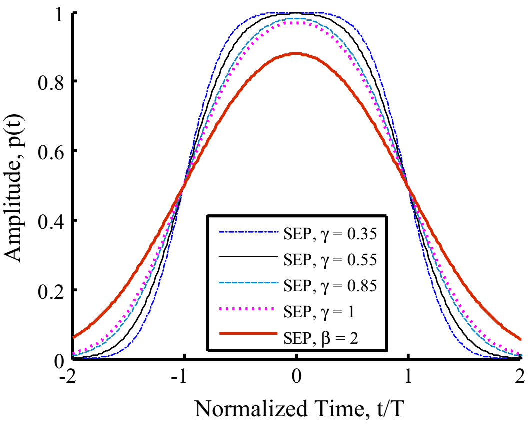

Fig. 4 Time function of SEP for $\alpha = 0.22$, with $\beta = 1$ when γ varies, and $\gamma = 0.55$ for $\beta = 2$

duration period; moreover, its amplitude is considerably minimized, attenuating the data symbols and increasing the BER. This is the main reason why we didn't consider implementing the SEP pulse with a high β.

The comparison of the frequency functions of the SPLP, and SPEP [19], IMBH [23], and IPLCP [24] with the proposed SEP pulse is shown in Fig. 5. The SEP possesses the smallest side lobes among the evaluated pulses. It is observed that pulse with a broader main lobe produces comparatively larger side lobes. Moreover, a balance between smaller side lobes and a broader main lobe is required for a pulse to perform better in terms of ICI power, PAPR, and BER. Moreover, a reduction in ICI power and PAPR are related to smaller magnitude side lobes [14], while the BER is related to a wider main lobe [15]. Though, it can see in Fig. 3 that $\gamma = 1$ produces smaller side lobes, but narrows the main lobe.

The comparison of different pulse shaping functions in the time domain is observed in Fig. 6. The IMBH showed the worst performance among the evaluated pulses, while SEP, SPLP and SPEP show better performance by preserving the time-domain rectangular behavior. The IPLCP and IMBH show small amplitude waveforms in the time-domain, and is characterized by a triangular shape waveform.

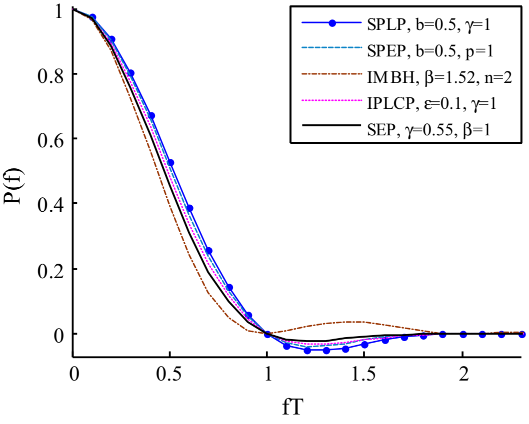

Fig. 5 Frequency function of various pulses for $\alpha = 0.22$

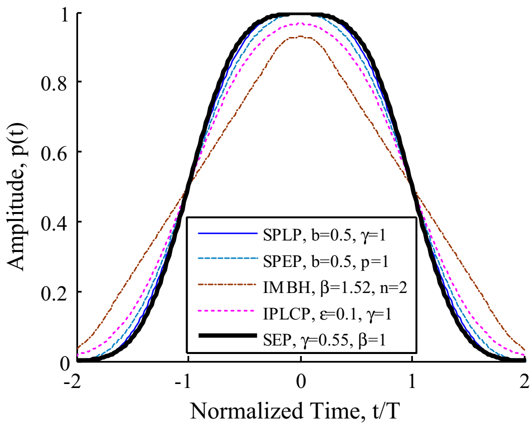

Fig. 6 Time function of various pulses for $\alpha = 0.22$

The behavior of the SEP was examined using two methods. First, we fixed $\beta = 1$ and changed the value of γ. This shows that the magnitude of the side lobe become smaller as γ increases. This observation gives the significance of γ. Second, we established $\gamma = 0.55$ and varied the value of β. In such scenario, it is observed that an increase in β, allows the main lobe be narrower. This observation points out the importance of the constant β. The design parameters for the SPLP, SPEP, IMBH, and IPLCP are the ones that exhibit the performance for OFDM systems and are given in [19, 23, 24]. Therefore, we implemented these values in our numerical and theoretical simulations to evaluate and compare the performance of the SPLP, SPEP, IMBH and IPLCP with the proposed SEP. In general, the SEP is more flexible in providing a broader main lobe with sufficiently reduced tail size.

4 Performance Evaluation

In this work, we employed the proposed SEP and other existing pulses in an OFDM-based system to evaluate and compare their performance in terms of ICI power, SIR power, BER, and PAPR via numerical and theoretical simulations. We found $\gamma = 0.55$ and $\beta = 1$ as the sub-optimum values for the SEP for $\alpha = 0.22$ after running extensive computer simulations. Therefore, these values are used, throughout the manuscript. Notice that, there is an optimum value of γ and β for every roll-off factor and transmission scheme, although it might not be unique.

First, we implemented a real OFDM-based system over an AWGN channel to compare the performance of different pulse shaping functions in terms of ICI power and SIR via numerical simulations. Simulation parameters are detailed in Table 1. Two of the best performing pulses in the recent literature are considered in our investigations. The IMBH [23] exhibits superiority in performance over other conventional pulses in terms of ICI power reduction and improved BER. Recently, the IPLCP [24] showed better performance than other recommended pulses in terms of PAPR reduction for $\alpha = 0.22$ in OFDM-based systems.

The comparison of various pulse shaping functions in terms of ICI power is illustrated in Fig. 7. These functions are employed in a 64-subcarrier OFDM system with normalized frequency offset, ΔfT, to measure performance against ICI power. The SEP outperforms SPLP, SPEP, and IPLCP, while it performed similarly compared to the IMBH in terms of

Table 1 Simulation Parameters for ICI and SIR

Parameter	Value
Modulation	BPSK
Number of symbols	100
Number of subcarriers	64
Input data block size	52
Transmission bandwidth	20 MHz
Block sampling	10
Roll-off factor, α	0.22

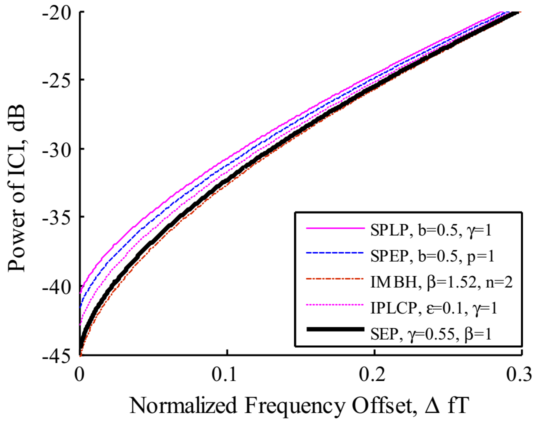

Fig. 7 ICI power of various pulses applied in a 64-subcarrier OFDM system, $\alpha = 0.22$

ICI power reduction. The proposed pulse showed relatively low ICI power for small and large normalized frequency offset. The SPLP presents the maximum ICI power among the evaluated pulses. This is because the SPLP has large magnitude side lobes, as shown in Fig. 5. The IMBH performs comparatively well with $n = 2$ in terms of ICI power reduction. However, SEP perform even better in terms of ICI power, if the value of γ or β is increased. Due to the tradeoff between ICI power and BER, we took only the sub-optimum values of the proposed pulse.

The SIR performance of various pulse shaping functions is illustrated in Fig. 8. The SEP performed well in terms of SIR power because it achieved the maximum SIR in comparison with the SPLP and SPEP [19], and IPLCP [24], The SIR power of the SEP is 27.92 dB for a normalized frequency offset, $\Delta fT = 0.15$, which is higher than the IPLCP, SPEP, and SPLP at 27.62, 27.18, and 26.62 dB, respectively, but lower than the IMBH at 28.46 dB. For a normalized frequency offset $\Delta fT = 0.35$, the SEP has a SIR power equal to 15.68 dB; while the IMBH, IPLCP, SPEP, and SPLP pulses obtained 15.81, 15.50, 15.31 and 15.12 dB, respectively. In general, the SEP performs similarly to the IMBH, while it performs better in comparison to the other pulses in terms of ICI and SIR power for a 64-subcarrier OFDM system.

Next, we evaluate the BER of the proposed pulse and other pulses in the presence of carrier frequency offset, carrier phase noise, and average ICI power. The theoretical expressions used to calculate the BER are given as follows [28]

$$\bar{B}\bar{E}\bar{R}_{OFDM} = 1 - (1 - BER_{symbol})^{N}, \tag{15}$$

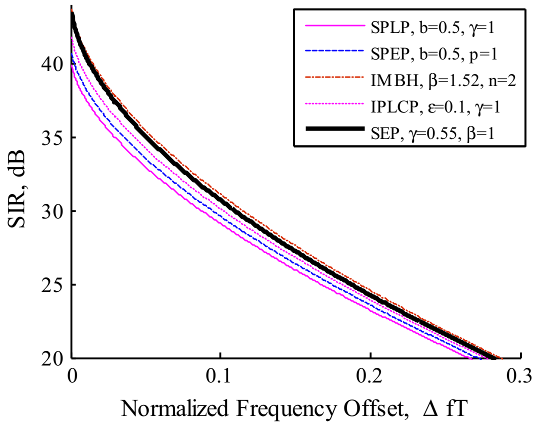

Fig. 8 SIR power of various pulses applied in a 64-subcarrier OFDM system, $\alpha = 0.22$

$$BER_{symbol} = \frac{1}{2}\left(Q(\cos\theta[P(-\Delta f) + \sqrt{P_{ICI}}]\sqrt{2\gamma_b}) + Q(\cos\theta[P(-\Delta f) - \sqrt{P_{ICI}}]\sqrt{2\gamma_b})\right). \tag{16}$$

where the average BER is given as a function of carrier frequency offset, Δf, carrier phase noise, θ, average ICI power, P_{ICI}, Fourier transform of the pulse shaping function, $P(f)$, the number of subcarriers, N, and $\gamma_b = E_b/N_0$. We employed different pulse shaping function in a 64-subcarrier BPSK-OFDM systems over an AWGN channel with $\Delta fT = \{0.15, 0.3\}$, and $\theta = \{10°, 30°\}$ for $\alpha = 0.22$ using (15) and (16) to measure BER via theoretical simulations.

The SEP has the lowest energy per bit-to-noise power spectral density ratio, E_b/N_o, value for a BER equal to 10^{-4} at $\Delta fT = 0.15$ compared to other existing pulses, as shown in Fig. 9. Whereas, the IMBH [23] has the worst performance in terms of BER. This is because it possesses a narrower main lobe compared to the other pulses, as shown in Fig. 5. The SPLP and SPEP [19] show good performance, but are outperformed by the SEP. In general, SEP, SPLCP, and SPEP completely outperform IMBH and IPLCP in terms of BER for low and high normalized frequency offsets. Figure 10 shows that when the value of the normalized frequency offset increases, the SEP presents even better performance by

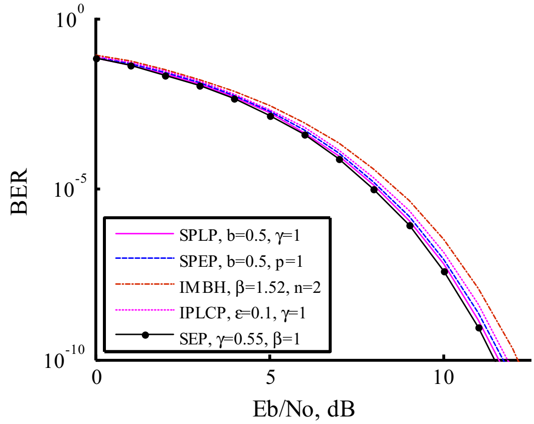

Fig. 9 BER performance comparison of different pulses in BPSK-OFDM system with $\Delta fT = 0.15$, $\theta = 10°$

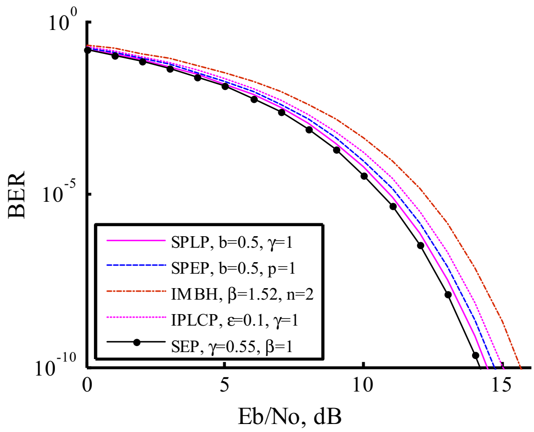

Fig. 10 BER performance comparison of various pulses in a BPSK-OFDM system with $\Delta fT = 0.3$, $\theta = 30°$

Table 2 Simulation Parameters for PAPR

Parameter	Value
Technology	OFDM
Modulation scheme	16-QAM
Number of subcarriers	256
Input data block size	64
Transmission bandwidth	20 MHz
Block oversampling	4
Uniform random data points	10^5
Roll-off factor, α	0.22

achieving lower BER values compared to the other pulses for $\Delta fT = 0.3$ and $\theta = 30°$. These results verify the superiority of the SEP over other existing pulses in terms of BER.

Finally, we evaluate and compare the performance of the proposed SEP with other existing pulses in terms of PAPR. We measured the PAPR value on the spectrum of the SEP and other pulse shaping functions, as it was done in [5, 24]. We simulate 10^5 systems blocks in a OFDM-based system to measure the total PAPR value at the transmitter side, which is determined by the combination of the pulse shaping function and the technology scheme. To reduce PAPR in OFDM system, a pulse shaping filter should be designed with small magnitude side lobe [5, 17, 24]. It is observed that SEP has the smallest side lobes among the evaluated pulses, as shown in Fig. 5. Table 2 shows the parameters implemented in our simulation to measure the PAPR of the different evaluated pulses.

The comparison of different pulse shaping functions in terms of PAPR reduction for OFDM-based systems using 16-QAM modulation is depicted in Fig. 11. The data is presented as an empirical complementary cumulative distribution function (CCDF), which measures the probability that the transmitted signal's PAPR exceeds a certain threshold, defined as $PAPR_0$. The proposed pulses SEP, SPLP and SPEP show superiority in performance over the IMBH [23] and IPLCP [24] in terms of the PAPR reduction. The SEP achieved the lowest PAPR value among the evaluated pulses, whereas SPLP and SPEP performed better by achieving smaller $PAPR_0$ values than the IMBH and IPLCP pulses.

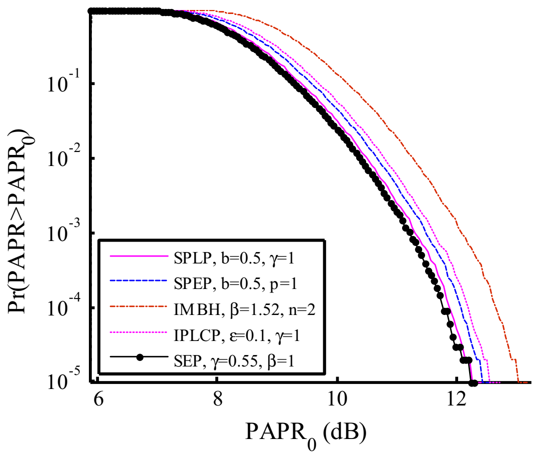

Fig. 11 CCDF of PAPR for various pulses applied in an OFDM system using 16-QAM

The IMBH pulse showed the worst performance in PAPR reduction among the evaluated pulses.

5 Complexity Evaluation

A pulse shaping function with a simple design and expression is extremely important for OFDM-based systems. This is because an inverse discrete Fourier transform (IDFT) is used in OFDM-based systems to transform the subcarrier amplitudes into a complex time domain signal. Next, a convolution operation takes place between the modulated symbols and the pulse shaping function. Further, the pulse shaping function of the proposed SEP has a simple expression compared to other existing pulses. Moreover, a pulse shaping function with a simple closed form expression is desired to reduce the complexity of the convolution process between the transmitted signal and the pulse shaping function in the system [29].

The time complexity of the convolution operation between the transmitted sequence and the pulse shaping pulse is evaluated using MATLAB's tic and toc commands [30]. The average elapsed time is estimated for the SEP, SPLP and SPEP [19], IMBH [23] and IPLCP [24]. When the tic command is executed, a function records an internal time of a computer system by running a stopwatch timer, and displays elapsed time in seconds at the execution of toc command. In-addition, these commands are used to estimate the elapsed time taken by a particular set of instructions to complete.

Table 3 Computer system specification

Title	Technology
Processor	Intel(R) Core(TM)2 Duo CPU E7400
Speed	2.80 GHz
System type	X86-based PC
RAM	4 GB
Windows	Microsoft Windows 7 Professional

Table 4 Average elapsed time of convolution

Pulse	Convolution (s)
SEP	4.8×10^{-5}
SPLP	5.1×10^{-5}
SPEP	5.6×10^{-5}
IMBH	6.2×10^{-5}
IPLCP	7.4×10^{-5}

The average elapsed time may vary depending on the specifications of the computer system used to execute tic and toc commands. We used a computer system with specifications given in Table 3. Table 4 illustrates the average elapsed time of the convolution process involving different pulse shaping functions. The SEP has the lowest average elapsed time compared to the other pulses. Therefore, it possesses the least complex impulse response function and it is suitable for OFDM-based systems. This is because it reduces the complexity of the convolution operation. As a result, the complexity of the convolution operation between the modulated symbols and the SEP is reduced. Whereas the IPLCP and IMBH present the highest average elapsed time due to complex pulse shaping functions.

6 Conclusion

A new family of Nyquist-I pulses known as sinc exponential pulse (SEP) is derived using the product of an exponential expression and a modified similar raised-cosine pulse. The SEP is characterized by two new design parameters, where γ increases the exponential power of the required function and β controls the phase of the modified sinc function. The sub-optimum values of the new design parameters are taken after running extensive computer simulations: $\gamma = 0.55$ and $\beta = 1$ for a roll-off factor, $\alpha = 0.22$. The pulse shaping function of the SEP is characterized by a simple closed form expression that reduces time complexity in OFDM systems. Simulation results verify that the SEP performs better than other existing pulses in terms of ICI power, SIR, BER, and PAPR for OFDM-based systems. In general, the proposed pulse has a great potential with respect to ICI power and PAPR reduction for OFDM-based systems and can effectively contribute to future wireless communication systems.

Acknowledgements This research was supported by the MSIP (Ministry of Science, ICT and Future Planning), Korea, under the ITRC (Information Technology Research Center) support program (IITP-2016-H8501-16-1007) supervised by the IITP (Institute for Information and Communications Technology Promotion). This research was supported by the MSIP (Ministry of Science, ICT and Future Planning, Korea, under the ITRC (Information Technology Research Center) support program (IITP-2016-R2718-16-0012) supervised by the IITP (National IT Industry Promotion Agency). This work was supported in part by Project FONDECYT No. 11160517, Fondo Nacional de Desarrollo Cientifico y Tecnolgico.

References

1. Hwang, T., Yang, C., Wu, G., Li, S., & Li, G. Y. (2009). OFDM and its wireless applications: A survey. *IEEE Transactions on Vehicular Technology, 58*(4), 1673–1694.
2. Rohling, H. (2011). *OFDM: Concepts for future communication systems*. Berlin: Springer.

3. Roh, W., Seol, J. Y., Park, J. H., Lee, B. H., Lee, J. K., Kim, Y. S., et al. (2014). Millimeter-wave beamforming as an enabling technology for 5G cellular communications: theoretical, feasibility and prototype results. *IEEE Communications Magazine, 52*(2), 106–113.
4. Chen, S., & Zhao, J. (2014). The requirements, challenges, and technologies for 5G of terrestrial mobile telecommunication. *IEEE Communications Magazine, 52*(5), 36–43.
5. Azurdia-Meza, C. A., Lee, K. J., & Lee, K. S. (2012). PAPR reduction by pulse shaping using Nyquist linear combination pulses. *IEICE Electronics Express, 9*(19), 1534–1541.
6. Hamdi, K. A. (2010). Exact SINR analysis of wireless OFDM in the presence of carrier frequency offset. *IEEE Transactions on Wireless Communications, 9*(3), 975–979.
7. Pan, W., Han, Y., Deng, G., & Zhong, P. (2015). Performance analysis of two-path transmission technique for intercarrier interference cancellation in OFDM systems. In *Proceedings of IEEE 26th annual international symposium on personal, indoor, and mobile radio communications* (pp. 55–60).
8. Bishnu, A., Jain, A., & Shrivastava, A. (2013). A new scheme of ICI self-cancellation in OFDM system. In *Proceedings of IEEE international conference on communication systems and network technologies* (pp. 120–123).
9. Kabil, S., Elassali, R., Elbahhar, F., Ouahman, A. A., & Essaid, B. A. (2014). Performance analysis of Doppler shift impact on the MB-OFDM system applied for vehicle to infrastructure communication. In *Proceedings of IEEE international conference on ultra-wideband* (pp. 433–437).
10. Goel, A. (2013). Phase rotated ICI self-cancellation scheme with frequency diversity for OFDM systems. In *Proceedings of IEEE International Conference on Signal Processing and Communication* (pp. 36–41).
11. Zhang, Z., & Ma, M. (2011). Research on pilot-aided channel estimation techniques in OFDM system. In *Proceedings of IEEE 7th international conference on wireless communications, networking and mobile computing* (pp. 1–4).
12. Venkatesan, S., & Valenzuela, R. A. (2016). OFDM for 5G: Cyclic prefix versus zero postfix, and filtering versus windowing. In *Proceedings of IEEE international conference on communications* (pp. 1–5).
13. Jiang, Y., Zhu, X., Lim, E. G., Huang, Y., & Lin, H. (2014). Low-complexity frequency synchronization for ICA based semi-blind CoMP systems with ICI and phase rotation caused by multiple CFOs. In *Proceedings of IEEE international conference on communications* (pp. 4571–4576).
14. Kumbasar, V., & Kucur, O. (2007). ICI reduction in OFDM systems by using improved sinc power pulse. *Elsevier Digital Signal Processing, 17*(6), 997–1006.
15. Alexandru, N. D., & Onofrei, A. L. (2009). ICI reduction in OFDM systems using phase modified sinc pulse. *Wireless Personal Communications, 53*(1), 141–151.
16. Tan, P., & Beaulieu, N. C. (2009). Analysis of the effects of Nyquist pulse-shaping on the performance of OFDM systems with frequency offset. *European Transactions on Telecommunications, 20,* 9–22.
17. Azurdia-Meza, C. A., Lee, K. J., & Lee, K. S. (2012). PAPR reduction in SC-FDMA by pulse-shaping using parametric linear combination pulses. *IEEE Communication Letters, 16*(12), 2008–2011.
18. Beaulieu, N. C., & Damen, M. O. (2004). Parametric construction of Nyquist-I pulses. *IEEE Transactions on Communications, 52*(12), 2134–2142.
19. Kamal, S., Azurdia-Meza, C. A., & Lee, K. S. (2015). Nyquist-I pulses designed to suppress the effect of ICI power in OFDM systems. In *Proceedings of IEEE 11th international wireless communications and mobile computing conference* (pp. 1412–1417).
20. Tan, P., & Beaulieu, N. C. (2005). Effect of transmitter Nyquist shaping on ICI reduction in OFDM systems with carrier frequency offset. *Electronics Letters, 41*(13), 746–748.
21. Tan, P., & Beaulieu, N. C. (2004). Reduced ICI in OFDM systems using the "Better Than" Raised-Cosine Pulse. *IEEE Communications Letters, 8*(3), 135–137.
22. Murad, H. M. (2006). Reducing ICI in OFDM systems using a proposed pulse shape. *Wireless Personal Communications, 40*(1), 41–48.
23. Saxena, R., & Joshi, H. D. (2013). ICI reduction in OFDM system using IMBH pulse shapes. *Wireless Personal Communications, 71*(4), 2895–2911.
24. Azurdia-Meza, C. A., Arrano, H. F., Estevez, C., & Soto, I. (2015). Performance enhancement of OFDM-based systems using improved parametric linear combination pulses. *Wireless Personal Communications, 85*(3), 809–824.
25. Third Generation Partnership Project (3GPP). (2014). Universal Mobile Telecommunications System (UMTS); Base station (BS) radio transmission and reception FDD. *European Telecommunications Standards Institute*, Tech. Rep. 125.104, 2014.
26. Third Generation Partnership Project (3GPP). (2014). Universal Mobile Telecommunications System (UMTS); User equipment (UE) radio transmission and reception FDD. *European Telecommunications Standards Institute*, Tech. Rep. 125.101, 2014.

27. Pollet, T., Bladel, M. V., & Moeneclaey, M. (1995). BER sensitivity of OFDM systems to carrier frequency offset and wiener phase noise. *IEEE Transactions on Communications, 43*(2/3/4), 191–193.
28. Le, K. N. (2008). Insight on ICI and its effects on performance of OFDM systems. *Digital Signal Processing, 18*(6), 876–884.
29. Kamal, S., Azurdia-Meza, C. A., & Lee, K. (2016). Suppressing the effect of ICI power using dual sinc pulses in OFDM-based systems. *AEÜ International Journal of Electronics and Communications, 70*(7), 953–960.
30. Solomon, C., & Breckon, T. (2011). *Fundamentals of digital image processing: a practical approach with examples in matlab*. Hoboken: Wiley-Blackwell.

Shaharyar Kamal received his B.S. degree in Software Engineering from City University of Science and Information Technology, Peshawar, Pakistan and M.S. degree in Computer Engineering from Mid Sweden University, Sweden. He is currently enrolled as Ph.D. candidate in the Department of Radio and Electronics Engineering at Kyung Hee University, Republic of Korea. His research interest includes advanced wireless communication systems, image and signal processing techniques, LTE Uplink Technology, Nyquist-I Pulses and Internet of Things for E-health.

Cesar A. Azurdia-Meza received the B.Sc. degree in electrical engineering from Universidad del Valle de Guatemala, Guatemala in 2005, and the M.Sc. degree in electrical engineering from Linnaeus University, Sweden in 2009. In 2013 he obtained the Ph.D degree in Electronics and Radio Engineering, Kyung Hee University, Republic of Korea. He joined the Department of Electrical Engineering, University of Chile as an Assistant Professor in August 2013. He has served as Technical Program Committee (TPC) member for multiple conferences, as well as a reviewer in journals such as IEEE Communications Letter, IEEE Transactions on Wireless Communications, Wireless Personal Communications, and EURASIP Journal on Advances in Signal Processing. Dr. Azurdia is an IEEE Communications Society Member, as well as IEICE Member. His research interests include topics such as Nyquist's ISI criterion, OFDM-based systems, SC-FDMA, visible light communication systems, 5G and beyond enabling technologies, and signal processing techniques for communication systems.

Kyesan Lee received a B.E. degree in electrical engineering from Kyung Hee University in Korea and M.S. and Ph.D. degrees from the department of electrical engineering, Keio University, Yokohama, Japan, in 1996, 1999, and 2002, respectively. He joined KDDI R&D Laboratories Inc in 2002 and has received the IEEE VTS Japan Young Researchers Encouragement Award. Since 2003, he has been with the College of Electronic and Information, Kyung Hee University, where he is a Professor. He received the excellent paper award in the 2009 IEEE ISCIT (international symposium on communication and information technology). He has received the Prime Minister Award in 2009. He received the Minister Award from the Ministry of Education Science and Technology in 2009. His research interests include wireless communication networks, CDMA, OFDM, MC-CDMA, MC-DS/CDMA, MIMO, and Cognitive radio and Visible Light Communication systems.